2014

DIGITAL STATE SPACE CONTROL OF THE QUADRUPLE-TANK PROCESS

Daniel T. Desautel
University of Rhode Island, djdtthomas@aol.com

DIGITAL STATE SPACE CONTROL OF THE QUADRUPLE-TANK PROCESS

BY

DANIEL T DESAUTEL

A THESIS SUBMITTED IN PARTIAL FULFILLMENT OF THE REQUIREMENTS FOR THE DEGREE OF

MASTER OF SCIENCE

IN

MECHANICAL ENGINEERING

UNIVERSITY OF RHODE ISLAND

2014

MASTER OF SCIENCE THESIS

OF

DANIEL T DESAUTEL

APPROVED:

Thesis Committee:

Major Professor Richard J. Vaccaro

Musa Jouaneh

David Chelidze

Nasser H. Zawia

Dean of the Graduate School

UNIVERSITY OF RHODE ISLAND

2014

ABSTRACT

The research represented in this thesis pertains to applying digital control to that of a Quadruple-Tank Process via implementation of State-Space theory. Having arranged the tank apparatus into the desired configurations of both the Coupled and Quadruple-Tank Processes, a mathematical model was applied that properly represented each systems' dynamics. From these dynamical equations linearized state-space models were formed, which would be the basis for computer aided control and simulation. Through software application of a linear state feedback tracking system both tank processes were able to be successfully controlled. Complex control issues regarding plant saturation and *integrator wind-up* are addressed giving way to a more responsive system that is stable under a larger range of unanticipated modeling errors. Analysis of the systems performance has shown good results in both simulation and experimental application to the Quanser Lab Tank Systems.

ACKNOWLEDGMENTS

This work would not have been possible without the continued support of my major advisor, Professor Richard J. Vaccaro. His willingness to guide me in the journey through my graduate studies has afforded me the opportunity to continue learning at a higher level. The instruction he has supplied over the past two years has answered many elusive questions. Through his teachings my perspective on the aspects of control have become substantially more thorough, and for that I am grateful.

I also wish to thank both of my committee chair members, Professor Musa Jouaneh and Professor David Chelidze. Their comments have improved both the level of understanding this thesis will bring to the outside reader and have shown me what is entailed when presenting material at a professional level.

I look now to continue my education in industry, where I may institute the teachings learned in academia toward real world problems.

TABLE OF CONTENTS

Page

LIST OF TABLES

LIST OF FIGURES

CHAPTER 1

Introduction

The Quadruple-Tank Process is a system which involves an interconnection of four fluid tanks. Each of these tanks has an orifice located in the bottom so that fluid may drain by way of gravity. These orifices are removable and constructed with various diameters allowing the system to have different sets of parameters. In this arrangement the tanks are split into two vertical sets so that one tank is positioned over another allowing fluid to drain from one tank to the second and then finally to a basin for recycling. The fluid flow from two positive displacement pumps is split between an upper tank and the opposing sets bottom tank as shown in Figure 1 [1]. The main focus of this system is to mandate the height of fluid in the bottom two tanks via a control system. This control system uses the tanks current fluid height as input to make proper height adjustments by varying the output of pump voltage, which imparts an inlet flow to the tanks.

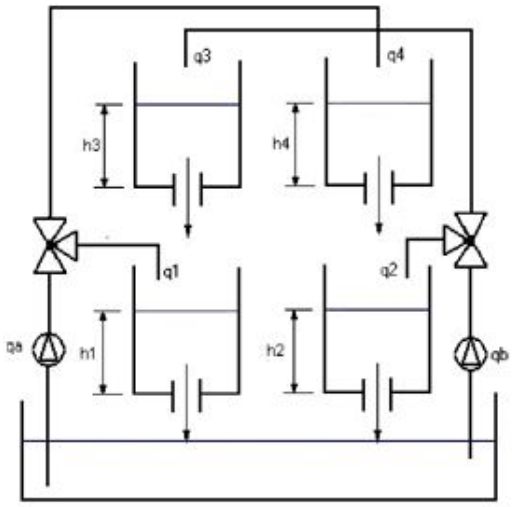

Figure 1. Schematic of Quadruple Tank Process and Parameter Values.[1]

Since its introduction in 1996 at the Lund Institute of Technology, Sweden the Quadruple-Tank Process (QTP) has been influential in illustrating several aspects of multi-variable control. Among these significant contributions is the systems ability to demonstrate the effects that multi-variable zero locations can cause in control design [2]. The traditional procedure for controlling the QTP has involved the use of predictive control, also referred to as cascade control. This mode of control is common because of its ability to actively adapt to both restrictions in modeling and physical capabilities of a system.

In predictive control the measured output from a system is fed to a control algorithm, which through a variety of methods attempts to predict the future state of the system given its current trajectory. The controller then adjusts the systems inputs in a manner to best satisfy the system approaching the desired state [3]. The desired result is a control system which responds faster than that of a standard feedback loop. However, this system is predicated on the accuracy and efficiency of the algorithm to predict the systems future state.

This current study seeks to employ digital state-space control on the QTP in the form of a full state feedback tracking system. In doing so the non-linear dynamics of the plant system will be linearized about an equilibrium point allowing a linear model to be introduced for analysis. Proper pole placement, gain calculation and stability will then be considered in order to produce both a working simulation in software as well as a working hardware model.

The hardware model used is constructed by Quanser Consulting and is commercially available as an open platform experimental apparatus. It is supplied with the necessary hardware items such as the pumps, amplifier, tanks and orifices to design a variety of tank processes. Also supplied with the module is the software drivers to interface between the control system and pressure sensors.

Furthermore, the QTP is representative of a higher order multi-variable control problem whose characteristics are inherent in a wide array of other applications. Topics discussed in this research will have a far reaching scope beyond the limits of this model. In order to facilitate a more complete understanding of the fundamental factors at work, a simplification of the QTP is first examined. This simplification being the Coupled-Tank System or CTP. This system shares similar dynamics with the QTP, but the order of difficulty is reduced in the sense that there are two tanks and only one pump to source a single inlet flow. The key aspects discovered in the CTP are thus able to be carried over into the QTP.

Included in this study is the discussion of Integrator Windup, a scenario where the integrator of the control system integrates the error function faster than the system can respond, essentially commanding the system to act beyond its physical means [4]. This is represented in the QTP system by the commanded pump output voltage. The pump itself has a limited operating range and techniques have to be implemented to avoid saturation. This condition of *integrator windup* is a commonly misunderstood concept of control theory and yet it must be accounted for in almost every controller that uses an integrator. Further understanding of this phenomena and methods to counteract its effects are in high demand and thus discussed in the following report.

CHAPTER 2

Model Development and Auto-Calibration

2.1 Coupled Tank System Dynamics

The coupled tank apparatus can be described by a 2nd order non-linear state space model. The state variables for this system are represented by the level of liquid in each tank as follows:

$$x_1 = \text{liquid level upper tank 1} \tag{2.1.1}$$
$$x_2 = \text{liquid level bottom tank 2}$$

In order to accurately model the physical characteristics of the system a basic mass rate balance is performed relating the rate of fluid both entering and exiting each respective tank. This equates to the overall rate of tank fluid level change represented by $\dot{x_1}$ and $\dot{x_2}$.

$$\text{Change in Tank Fluid Height} = \text{Mass Rate In - Mass Rate Out}$$
$$\dot{x_1} = \beta_1 u_1 - \alpha_1 \sqrt{2gx_1} \tag{2.1.2}$$
$$\dot{x_2} = \alpha_1 \sqrt{2gx_1} - \alpha_2 \sqrt{2gx_2}$$

Here g represents the acceleration due to gravity. β_1 is the pump coefficient and u is the input voltage to the pump. Both α_1 and α_2 represent the respective tank orifice coefficients. Note that the model shows a nonlinear relation between the height of liquid in the tank and the rate at which it empties.

2.1.1 Coupled Tank Linearization

In order to apply linear control theory to this nonlinear system the model must first be linearized. This is accomplished by selecting an equilibrium point about

which to linearize. A linear approximation such as this becomes less accurate the further away from the equilibrium point the system goes. Considering that each tank has a maximum height of 30 cm an equilibrium of 15 cm is chosen for tank one to best minimize the severity of error at both extremes of the tank. The equilibrium height for tank two can then be calculated.

$$x_e = \begin{bmatrix} x_e(1) \\ x_e(2) \end{bmatrix} = \begin{bmatrix} 15 \\ x_e(2) \end{bmatrix}. \tag{2.1.3}$$

This constant equilibrium vector can then be plugged into the tank level rate Equation 2.1.2 with $u = u_e$, an unknown constant equilibrium pump voltage. With the constant tank height mandated the rate of change of heights is zero.

$$\begin{aligned} 0 &= \beta_1 u_e - \alpha_1 \sqrt{2g x_e(1)} \\ 0 &= \alpha_1 \sqrt{2g x_e(1)} - \alpha_2 \sqrt{2g x_e(2)} \end{aligned} \tag{2.1.4}$$

Rearranging terms of the first equation yields the equilibrium pump voltage, or plant input:

$$u_e = \frac{\alpha_1 \sqrt{2g x_e(1)}}{\beta_1} \tag{2.1.5}$$

A similar rearrangement of the second equation yields the equilibrium height of tank two:

$$x_e(2) = \frac{{\alpha_1}^2 x_e(1)}{{\alpha_2}^2} \tag{2.1.6}$$

The linear control system implemented will control deviations of the plant state variables from the selected equilibrium point. In order to obtain a linear state space model for the deviations, let

$$x = x_e + w, \text{ or } x_1 = x_e(1) + w_1 \text{ and } x_2 = x_e(2) + w_2 \tag{2.1.7}$$

Here w is a vector of deviations from the equilibrium tank liquid levels. Similarly, deviations in the pump voltage, or plant input, from its equilibrium value can be

modeled using a deviation term v.

$$u = u_e + v \tag{2.1.8}$$

Substituting these equations, which account for deviations from equilibrium, back into the original state space model yields:

$$\begin{aligned} \dot{w_1} &= \beta_1(u_e + v) - \alpha_1\sqrt{2gx_1} \\ \dot{w_2} &= \alpha_1\sqrt{2gx_1} - \alpha_2\sqrt{2gx_2} \end{aligned} \tag{2.1.9}$$

Using a Taylor series expansion of the square root functions in the previous equations, a linear approximation may be formed as follows:

$$\sqrt{2gx_1} \approx \sqrt{2gx_e(1)} + \sqrt{\frac{g}{2x_e(1)}}w_1 \tag{2.1.10}$$

Thus substituting this approximation into the state space model yields:

$$\begin{aligned} \dot{w_1} &= -\alpha_1\sqrt{2gx_e(1)} - \alpha_1\sqrt{\frac{g}{2x_e(1)}}w_1 + \beta_1 u_e + \beta_1 v \\ \dot{w_2} &= \alpha_1\sqrt{2gx_e(1)} + \alpha_1\sqrt{\frac{g}{2x_e(1)}}w_1 - (\alpha_2\sqrt{2gx_e(2)} + \alpha_2\sqrt{\frac{g}{2x_e(2)}}w_2) \end{aligned} \tag{2.1.11}$$

Using the steady state relations of Equation 2.1.4 the preceeding can be further simplified to:

$$\begin{aligned} \dot{w_1} &= -\alpha_1\sqrt{\frac{g}{2x_e(1)}}w_1 + \beta_1 v \\ \dot{w_2} &= \alpha_1\sqrt{\frac{g}{2x_e(1)}}w_1 - \alpha_2\sqrt{\frac{g}{2x_e(2)}}w_2 \end{aligned} \tag{2.1.12}$$

The linearized state-space model that describes the deviations from the equilibrium point is

$$\begin{bmatrix} \dot{w_1} \\ \dot{w_2} \end{bmatrix} = \begin{bmatrix} -\lambda_1 & 0 \\ \lambda_1 & -\lambda_2 \end{bmatrix} \begin{bmatrix} w_1 \\ w_2 \end{bmatrix} + \begin{bmatrix} \beta_1 \\ 0 \end{bmatrix} v \tag{2.1.13}$$

where

$$\lambda_1 = \alpha_1\sqrt{\frac{g}{2x_e(1)}}, \quad \lambda_2 = \alpha_2\sqrt{\frac{g}{2x_e(2)}} \tag{2.1.14}$$

2.2 Quadruple Tank System Dynamics

As an expansion of the coupled tank the quadruple tank system is represented by a 4th order nonlinear state space model. The state variables are thus expanded to include:

$$x_1 = \text{liquid level tank 1}$$

$$x_2 = \text{liquid level tank 2}$$

$$x_3 = \text{liquid level tank 3}$$

$$x_4 = \text{liquid level tank 4}$$

Performing a similar mass rate balance as was done on the coupled tank for the quadruple tank system reveals a nonlinear state space model as follows.

$$\begin{aligned}
\dot{x_1} &= \beta_1 u_1 - \alpha_1\sqrt{2gx_1} + \alpha_3\sqrt{2gx_3} \\
\dot{x_2} &= \beta_2 u_2 - \alpha_2\sqrt{2gx_2} + \alpha_4\sqrt{2gx_4} \\
\dot{x_3} &= \beta_3 u_2 - \alpha_3\sqrt{2gx_3} \\
\dot{x_4} &= \beta_4 u_1 - \alpha_4\sqrt{2gx_4}
\end{aligned} \tag{2.2.1}$$

Here u_1 and u_2 represent two inputs to the system as voltages applied to pump one and pump two respectively. α and β values represent the orifice and pump coefficients for each tank. As before, this system has a non-linearity with regard to each tank emptying proportional to the square root of tank level height.

2.2.1 Quad Tank Linearization

The solution is then to choose an equilibrium point using a fixed input u_e to obtain a constant state vector x_e.

$$x_e = \begin{bmatrix} x_e(1) \\ x_e(2) \\ x_e(3) \\ x_e(4) \end{bmatrix}, u_e = \begin{bmatrix} u_{e1} \\ u_{e2} \end{bmatrix} \tag{2.2.2}$$

Inputing these equilibrium values into the state space model and assuming a steady state condition yields

$$\begin{aligned} 0 &= \beta_1 u_{e1} + \alpha_3\sqrt{2gx_e(3)} - \alpha_1\sqrt{2gx_e(1)} \\ 0 &= \beta_2 u_{e2} + \alpha_4\sqrt{2gx_e(4)} - \alpha_2\sqrt{2gx_e(2)} \\ 0 &= \beta_3 u_{e2} - \alpha_3\sqrt{2gx_e(3)} \\ 0 &= \beta_4 u_{e1} - \alpha_4\sqrt{2gx_e(4)} \end{aligned} \tag{2.2.3}$$

The elements of the constant state vector may now be solved through simple algebraic manipulation and substitution. These efforts together reveal the elements to be of the form:

$$\begin{aligned} x_e(1) &= \frac{1}{2g}(\frac{\beta_1 u_{e1} + \beta_3 u_{e2}}{\alpha_1})^2 \\ x_e(2) &= \frac{1}{2g}(\frac{\beta_2 u_{e2} + \beta_4 u_{e1}}{\alpha_2})^2 \\ x_e(3) &= \frac{1}{2g}(\frac{\beta_3 u_{e2}}{\alpha_3})^2 \\ x_e(4) &= \frac{1}{2g}(\frac{\beta_4 u_{e1}}{\alpha_4})^2 \end{aligned} \tag{2.2.4}$$

Having found the equilibrium point around which to linearize, a linear state space model can now be constructed, which approximately describes the deviations of the state variables and inputs from the equilibrium. Once again this is performed by equating the actual state vector x to that of the equilibrium state vector x_e

plus some vector of deviations w.

$$x(t) = x_e + w(t)$$

The plant input vector u can also be described in this manner as the sum of equilibrium plant input vector u_e and deviations vector v.

$$u(t) = u_e + v(t)$$

Substituting these terms into the non-linear state space returns the following.

$$\begin{aligned}
\dot{w_1} &= \beta_1(u_{e1} + v_1) - \alpha_1\sqrt{2gx_1} + \alpha_3\sqrt{2gx_3} \\
\dot{w_2} &= \beta_2(u_{e2} + v_2) - \alpha_2\sqrt{2gx_2} + \alpha_4\sqrt{2gx_4} \\
\dot{w_3} &= \beta_3(u_{e2} + v_2) - \alpha_3\sqrt{2gx_3} \\
\dot{w_4} &= \beta_4(u_{e1} + v_1) - \alpha_4\sqrt{2gx_4}
\end{aligned} \tag{2.2.5}$$

Linear approximations for the powered terms can be found using the first order expansion of the Taylor series as follows.

$$f(x) = (2gx)^{1/2} \approx \sqrt{2gx_e} + \sqrt{\frac{g}{2x_e}}(x - x_e)$$

or

$$\sqrt{2gx_e} + \sqrt{\frac{g}{2x_e}}w$$

Substituting these linear approximations back into the previously solved model with deviations from equilibrium yields

$$\begin{aligned}
\dot{w_1} &= \beta_1 u_{e1} + \beta_1 v_1 + \alpha_3\sqrt{2gx_e(3)} + \alpha_3\sqrt{\frac{g}{2x_e(3)}}w_3 - \alpha_1\sqrt{2gx_e(1)} - \alpha_1\sqrt{\frac{g}{2x_e(1)}}w_1 \\
\dot{w_2} &= \beta_2 u_{e2} + \beta_2 v_2 + \alpha_4\sqrt{2gx_e(4)} + \alpha_4\sqrt{\frac{g}{2x_e(4)}}w_4 - \alpha_2\sqrt{2gx_e(2)} - \alpha_2\sqrt{\frac{g}{2x_e(2)}}w_2 \\
\dot{w_3} &= \beta_3 u_{e2} + \beta_3 v_2 - \alpha_3\sqrt{2gx_e(3)} - \alpha_3\sqrt{\frac{g}{2x_e(3)}}w_3 \\
\dot{w_4} &= \beta_4 u_{e1} + \beta_4 v_1 - \alpha_4\sqrt{2gx_e(4)} - \alpha_4\sqrt{\frac{g}{2x_e(4)}}w_4
\end{aligned} \tag{2.2.6}$$

Referencing back to the elements of constant state vector x_e in Equation 2.2.3, it can be shown that these equilibrium relations simplify the above deviatoric equations to the following:

$$\begin{aligned}
\dot{w_1} &= \beta_1 v_1 + \alpha_3\sqrt{\frac{g}{2x_e(3)}}w_3 - \alpha_1\sqrt{\frac{g}{2x_e(1)}}w_1 \\
&= -\lambda_1 w_1 + \lambda_3 w_3 + \beta_1 v_1 \\
\dot{w_2} &= \beta_2 v_2 + \alpha_4\sqrt{\frac{g}{2x_e(4)}}w_4 - \alpha_2\sqrt{\frac{g}{2x_e(2)}}w_2 \\
&= -\lambda_2 w_2 + \lambda_4 w_4 + \beta_2 v_2 \\
\dot{w_3} &= \beta_3 v_2 - \alpha_3\sqrt{\frac{g}{2x_e(3)}}w_3 \\
&= -\lambda_3 w_3 + \beta_3 v_2 \\
\dot{w_4} &= \beta_4 v_1 - \alpha_4\sqrt{\frac{g}{2x_e(4)}}w_4 \\
&= -\lambda_4 w_4 + \beta_4 v_1
\end{aligned} \tag{2.2.7}$$

where

$$\lambda_1 = \alpha_1\sqrt{\frac{g}{2x_e(1)}}, \quad \lambda_2 = \alpha_2\sqrt{\frac{g}{2x_e(2)}}, \quad \lambda_3 = \alpha_3\sqrt{\frac{g}{2x_e(3)}}, \quad \lambda_4 = \alpha_4\sqrt{\frac{g}{2x_e(4)}}$$

From these simplified equations a linear state space model may be formed. This model will be the basis for the control of the Quadruple Tank.

$$\dot{w} = \begin{bmatrix} -\lambda_1 & 0 & \lambda_3 & 0 \\ 0 & -\lambda_2 & 0 & \lambda_4 \\ 0 & 0 & -\lambda_3 & 0 \\ 0 & 0 & 0 & -\lambda_4 \end{bmatrix} w + \begin{bmatrix} \beta_1 & 0 \\ 0 & \beta_2 \\ 0 & \beta_3 \\ \beta_4 & 0 \end{bmatrix} v \tag{2.2.8}$$

2.3 Automatic Dynamic Calibration

Due to uncontrollable variables such as barometric pressure and other environmental influences the sensors used in this system require calibration in order to

supply accurate information to the control system. This calibration is performed in a dynamic nature in order to best simulate the real world use of the sensor. It is known that the sensor responds to water pressure in a linear manner i.e. the voltage signal sent from the sensor is linearly proportional to the height of water acting on the sensor. The pressure sensors signal voltage thus follows the form:

$$x = g * SensorVoltage + b \tag{2.3.1}$$

Here the variable x correlates to the height of water in the respective tank where the variables g and b represent the gain and offset of the pressure sensor signal voltage. By experimentally calculating these values the pressure sensors of the system can be effectively zeroed yielding a much more accurate measurement of the system to be fed to the control law.

The dynamic calculation of these values is performed by commanding a fixed voltage to the pump, which in turn supplies a fixed volumetric rate of water to both tanks. After an arbitrarily long time the height in both tanks reach their steady state values. This value along with the pressure sensor voltage is recorded and the experiment is repeated with a new fixed pump voltage. Table 1 supplied below demonstrates the trend of data taken when the Quanser Consulting *medium* diameter orifices are inserted in both the upper and lower tanks of the CTP.

Pump Voltage (V)	Time to SS (s)	Height 1	Sensor 1	Height 2	Sensor 2
4	125	3.5cm	0.5864 V	3.25cm	0.2892 V
5	250	7.5cm	1.3422 V	7.25cm	1.0359 V
6	375	12.25cm	2.2396 V	12cm	1.9148 V
7	500	17.75cm	3.2051 V	17.75cm	2.8947 V

Table 1. Steady state tank fluid heights recorded at constant pump voltage

These four data points are then folded back into the linear equation solving

for g and b with a least squares method:

$$\begin{bmatrix} x_1 \\ x_2 \\ x_3 \\ x_4 \end{bmatrix} = \begin{bmatrix} v_1 & 1 \\ v_2 & 1 \\ v_3 & 1 \\ v_4 & 1 \end{bmatrix} \begin{bmatrix} g \\ b \end{bmatrix}$$

For an arbitrary matrix A: $[A]^L = (A^T A)^{-1} A^T$

$$\begin{bmatrix} v_1 & 1 \\ v_2 & 1 \\ v_3 & 1 \\ v_4 & 1 \end{bmatrix}^L \begin{bmatrix} x_1 \\ x_2 \\ x_3 \\ x_4 \end{bmatrix} = \begin{bmatrix} g \\ b \end{bmatrix}$$

Inputting the experimental values found in Table 1 into this linear relation reveals gain and offset values for pressure sensors 1 and 2 as follows:

$$\begin{bmatrix} 0.5864 & 1 \\ 1.3422 & 1 \\ 2.2396 & 1 \\ 3.2051 & 1 \end{bmatrix}^L \begin{bmatrix} 3.5 \\ 7.5 \\ 12.25 \\ 17.75 \end{bmatrix} = \begin{bmatrix} g_1 = 5.4310 \\ b_1 = 0.2391 \end{bmatrix} \tag{2.3.2}$$

$$\begin{bmatrix} 0.2892 & 1 \\ 1.0359 & 1 \\ 1.9148 & 1 \\ 2.8947 & 1 \end{bmatrix}^L \begin{bmatrix} 3.25 \\ 7.25 \\ 12 \\ 17.75 \end{bmatrix} = \begin{bmatrix} g_2 = 5.5558 \\ b_2 = 1.5420 \end{bmatrix} \tag{2.3.3}$$

These values can then be put back into the control system to properly scale the sensor voltage to tank height.

2.3.1 Calculating α and β

As previously discussed the governing equations that represent the dynamics of the Coupled Tank System are as follows:

$$\dot{x_1} = -\alpha_1 \sqrt{2gx_1} + \beta u$$

$$\dot{x_2} = \alpha_1 \sqrt{2gx_2} - \alpha_2 \sqrt{2gx_2}$$

When constant pump voltage $\bar{u}_1$ is supplied to the apparatus the height in Tank 1 and Tank 2 reach Steady State values $\bar{x}_1$ and $\bar{x}_2$. The resulting dynamics

then follow:

$$0 = -\alpha_1\sqrt{2g\bar{x}_1} + \beta\bar{u}_1$$

$$0 = \alpha_1\sqrt{2g\bar{x}_2} - \alpha_2\sqrt{2g\bar{x}_2}$$

In order to solve for the orifice coefficients α_1 and α_2 the pump coefficient β must first be found through a separate analysis. Blocking the orifice at the bottom of Tank 1 limits the dynamics to a single equation with only one unknown. This equation relates the input voltage and pump volumetric coefficient linearly to the change in tank fluid height.

$$\dot{x_1} = \beta\bar{u}_1$$

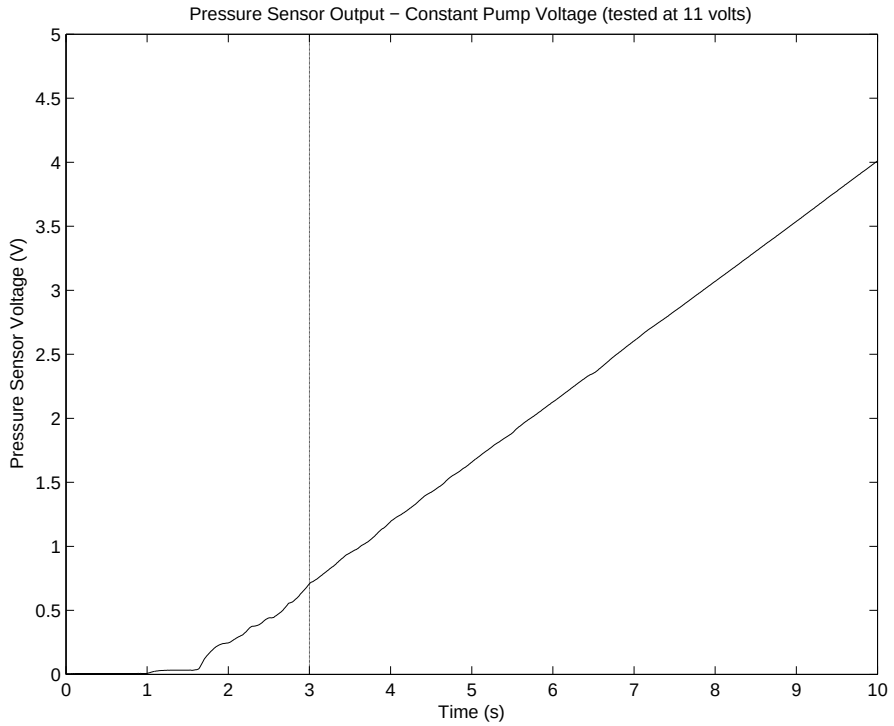

Figure 2. Sensor voltage of Tank 1 under constant inlet flow and no outlet flow.

By blocking the orifice of Tank 1 and applying a known fixed voltage to the pump, data from the pressure sensor can now be collected as shown in Figure 2. It is important to note that this voltage sensor data must first be scaled by the

gain and offset calculated previously in order for an accurate β calculation to be made. Performing this experiment at a constant voltage of 11 volts yields the linear data found in both Figure 2 and 3. Notice that due to the delay and turbulence experienced in the initial filling of the tank the first 3 seconds of data are stricken from this calculation. This cutoff represented in Figure 2 by the vertical line. Applying a linear fit to the cropped and calibrated data in Figure 3 reveals $\dot{x}$, which can then be divided by the constant voltage $\bar{u}_1$, or 11 volts, to solve for β.

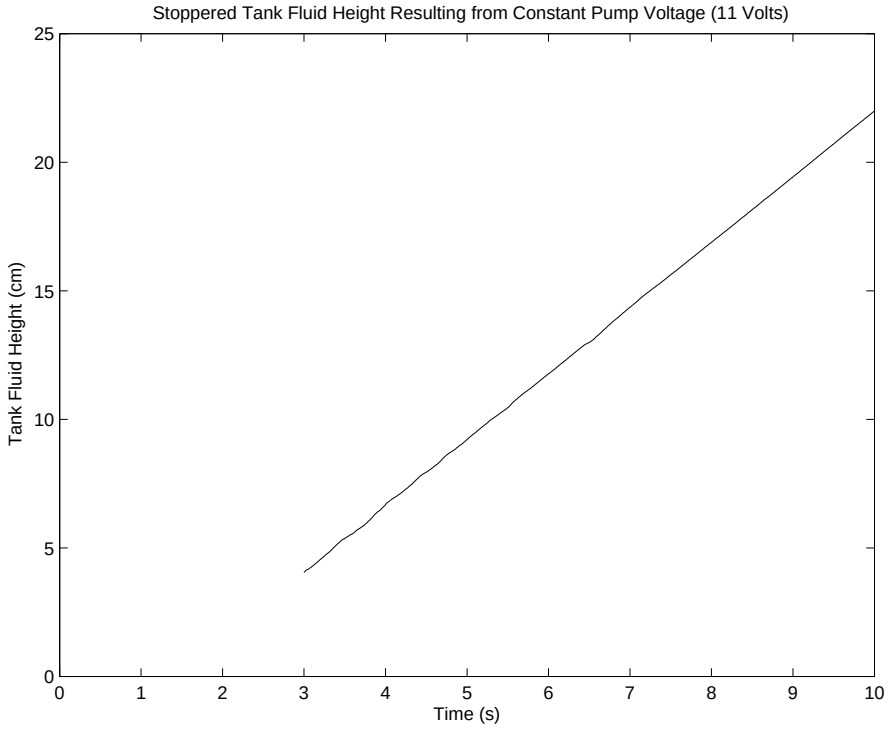

Figure 3. Calibrated sensor voltage to reflect fluid height of Tank 1 under constant inlet flow and no outlet flow.

Applying this methodology to the calibrated sensor data in Figure 3 yields a value of:

$$\beta = 0.24813$$

Calculation of α_1 and α_2 incorporates the data taken from Table 1 also used to calculate g and b earlier for sensor calibration. However this time the relation-

ship between the pump voltage and resulting steady state height in the tanks is important. Re-writing the steady state equations of 2.1.4 reveals:

$$\alpha_1\sqrt{2g\bar{x}_1} = \beta\bar{u}_1$$

$$\alpha_1\sqrt{2g\bar{x}_1} - \alpha_2\sqrt{2g\bar{x}_2} = 0$$

These steady state equations can be formulated into a linear system as follows utilizing each of the four recorded data points.

$$\begin{bmatrix} c_1 & 0 \\ c_1 & -c_3 \\ c_1 & 0 \\ c_1 & -c_3 \\ c_1 & 0 \\ c_1 & -c_3 \\ c_1 & 0 \\ c_1 & -c_3 \end{bmatrix} \begin{bmatrix} \alpha_1 \\ \alpha_2 \end{bmatrix} = \beta \begin{bmatrix} c_2 \\ 0 \\ c_2 \\ 0 \\ c_2 \\ 0 \\ c_2 \\ 0 \end{bmatrix}$$

where

$$c_1 = \sqrt{2g\bar{x}_1}$$

$$c_2 = \bar{u}_1$$

$$c_3 = \sqrt{2g\bar{x}_2}$$

Solving for α_1 and α_2:

$$\begin{bmatrix} c_1 & 0 \\ c_1 & -c_3 \\ c_1 & 0 \\ c_1 & -c_3 \\ c_1 & 0 \\ c_1 & -c_3 \\ c_1 & 0 \\ c_1 & -c_3 \end{bmatrix}^L \beta \begin{bmatrix} c_2 \\ 0 \\ c_2 \\ 0 \\ c_2 \\ 0 \\ c_2 \\ 0 \end{bmatrix} = \begin{bmatrix} 82.867 & 0 \\ 82.867 & -79.853 \\ 121.31 & 0 \\ 121.31 & -119.27 \\ 155.03 & 0 \\ 155.03 & -153.44 \\ 186.62 & 0 \\ 186.62 & -186.62 \end{bmatrix}^L 0.24813 \begin{bmatrix} 4 \\ 0 \\ 5 \\ 0 \\ 6 \\ 0 \\ 7 \\ 0 \end{bmatrix} = \begin{bmatrix} \alpha_1 \\ \alpha_2 \end{bmatrix}$$

$$\begin{bmatrix} \alpha_1 \\ \alpha_2 \end{bmatrix} = \begin{bmatrix} 0.0097909 \\ 0.0098811 \end{bmatrix}$$

Here the resulting values were: $\alpha_1 = 0.0097909$ and $\alpha_2 = 0.0098811$

Because of the structure of this dynamic calibration there exists a deviance of parameters each time they are calculated. As mentioned the pressure sensors are susceptible to deviation depending on ambient pressure on any given day. Also the pump's volumetric output β can vary slightly given changes in water viscosity, condition of seals and temperature. For these reasons the assumed constant α values will also change simply because of the manner in which they are calculated. Quanser Consulting issues constant values for the supplied orifices, but given the nature of the system the newly calibrated and calculated parameters yield good results when used together. The tables below demonstrate the deviation experienced during calibration over an arbitrarily long length of time. The tables are grouped by raw experimental and the parameters that were calculated as a result.

Pump Voltage (V)	Time to SS (s)	Height 1	Sensor 1	Height 2	Sensor 2
4	125	3.75cm	0.8044 V	3.5cm	0.1262 V
5	250	7.75cm	1.5890 V	7.5cm	0.9060 V
6	375	12cm	2.4885 V	11.75cm	1.7185 V
7	500	17cm	3.5150 V	17cm	2.6663 V

Table 2. Steady state tank fluid heights recorded at constant pump voltage - 1

Parameter	Value
α_1	0.0092892
α_2	0.0093759
β	0.2337
g_1	4.8693
b_1	-0.0968
g_2	5.3110
b_2	2.7415

Table 3. Parameter Values for the Quanser Lab Quadruple Tank Process - 1

Pump Voltage (V)	Time to SS (s)	Height 1	Sensor 1	Height 2	Sensor 2
4	125	3.75cm	0.6851 V	3.25cm	0.3134 V
5	250	7.5cm	1.4334 V	7cm	0.9491 V
6	375	11.5cm	2.2809 V	11cm	1.7293 V
7	500	16.75cm	3.2831 V	16.75cm	2.7400 V

Table 4. Steady state tank fluid heights recorded at constant pump voltage - 2

Parameter	Value
α_1	0.0098486
α_2	0.0099109
β	0.2457
g_1	5.2342
b_1	-0.1155
g_2	5.6023
b_2	1.7846

Table 5. Parameter Values for the Quanser Lab Quadruple Tank Process - 2

Pump Voltage (V)	Time to SS (s)	Height 1	Sensor 1	Height 2	Sensor 2
4	125	3.25cm	0.5565 V	3cm	0.0143 V
5	250	7cm	1.3023 V	6.75cm	0.7464 V
6	375	11.5cm	2.1669 V	11cm	1.5634 V
7	500	16.5cm	3.0661 V	16.5cm	2.4875 V

Table 6. Steady state tank fluid heights recorded at constant pump voltage - 3

Parameter	Value
α_1	0.0099184
α_2	0.0099811
β	0.2474
g_1	5.5177
b_1	-0.0935
g_2	5.6784
b_2	2.8914

Table 7. Parameter Values for the Quanser Lab Quadruple Tank Process - 3

Though not shown here the α and β values are calculated in a similar manner for the QTP. That is all tanks with an inlet flow have their orifices blocked in order

to calculate their respective β. The gain, offset and α values are then collected by examining the steady state heights as done with the CTP. Essentially the equations used in the CTP are extended to encompass the QTP.

CHAPTER 3

Coupled-Tank Process Control

3.1 Linear State-Feedback Tracking System

In order to mandate the fluid level in the bottom tank of the coupled-tank apparatus a control method must first be determined. Since all state variables, or tank fluid heights, are directly measured via pressure sensors full state-feedback may be implemented using the linearized dynamics of the system. Because the bottom tank fluid level will be a mandated series of step commands a tracking based system is selected. In such systems a reference input is supplied to the control algorithm and the output of the system is required to be equal, or close to the value of the reference input. This follows the concept that once the reference or commanded height of the bottom tank is designated the control algorithm will track the system until the output reaches that of the reference value.

As previously stated in Chapter 2 the dynamics of the system have been linearized around an equilibrium point so that a linear control scheme may be applied. Considering the fact that these equilibrium values are known the tracking system is then best suited to track the specified heights as they relate to the determined equilibrium. This is to say that the control system will *track* deviations from the equilibrium values.

3.1.1 State-Space Tracking System Architecture

A standard state-space tracking design may be created for the coupled tank system as introduced in [5]. An nth order linear, single input, single output plant has a state space model:

$$\dot{\mathrm{x}}(t) = \mathrm{A}\mathrm{x}(t) + \mathrm{b}u(t) \tag{3.1.1}$$
$$y(t) = \mathrm{c}\mathrm{x}(t)$$

Because the coupled tank process is controlled in discrete time the plant dynamics must be mapped into the z-plane using a zero order hold equivalent model. A zero order hold, or ZOH, model digitally represents an analog system with D/A and A/D converters operating with a sampling interval of T seconds. The equivalent model is produced through the following transformation of the plant:

$$\Phi = e^{AT} \tag{3.1.2}$$
$$\Gamma = \int_0^T e^{A\tau}\,\mathrm{d}\tau$$

For a sampling interval of T seconds the plant model then becomes:

$$x[k+1] = \Phi x[k] + \Gamma u[k] \tag{3.1.3}$$
$$y[k] = \mathrm{c}x[k]$$

where

$$x[k] = x(kT), \quad y[k] = y(kT)$$
$$\text{and}$$
$$u[k] = u(t), \quad kT \leq t \leq (k+1)T$$

Additional dynamics must be introduced to this model in order to obtain a design where $y[k]$ tracks the reference input r[k] with zero steady-state error. When cascaded with the plant dynamics these additional dynamics form an augmented

design plant that allows exact tracking to a specified zero-input trajectory [6]. Essentially from these additional dynamics a regulator is able to be formed that instead of attenuating to zero allows the plant output to attain mandated levels. The additional dynamics are represented by:

$$x_a[k+1] = \Phi_a x_a[k] + \Gamma_a u[k] \tag{3.1.4}$$
$$y_a[k] = \mathrm{c}x_a[k]$$

Here Φ_a includes the poles of the z transform of r[k]. For step-input tracking this is a pole at $z = 1$; that is, a digital integrator. The cascade architecture of the additional and plant dynamics may be seen in Figure 5. This cascade structure forms a design model that will be used to calculate the $1 \times n$ state-feedback gain vector L_1 and the integrator gain L_2. The design model is given by:

$$\Phi_d = \begin{bmatrix} \Phi & 0 \\ \Gamma_a \mathrm{c} & \Phi_a \end{bmatrix}, \Gamma_d = \begin{bmatrix} \Gamma \\ 0 \end{bmatrix} \tag{3.1.5}$$

Since the coupled tank system is representative of a SISO (Single Input Single Output) system a desired set of $n + 1$ closed loop poles may be selected to calculate the gain vector L_d using Matlab's *place* command. In standard fashion closed loop poles are chosen to be the roots of a n+1-order normalized Bessel polynomial, as shown in Table 8, scaled to the desired settling time, T_s. A settling time of 20 seconds is chosen for the CTP and the resulting calculation for its third-order design model takes the form:

$$\mathrm{eig}(\Phi_d - \Gamma_d L_d) = e^{T * s_3 / T_s} \tag{3.1.6}$$

L_1 consists of the first 2 elements of L_d, while the remaining element is the L_2 gain.

Variable	Pole Locations
s_1	-4.6200
s_2	$-4.0530, \pm j2.3400$
s_3	$-5.0093, -3.9668 \pm j3.7845$
s_4	$-4.0156, \pm j5.0723, -5.5281 \pm j1.6553$
s_5	$-6.4480, -4.1104 \pm j6.3142, -5.9268 \pm j3.0813$
s_6	$-4.2169 \pm j7.5300, -6.2613 \pm j4.4018, -7.1205 \pm 1.4540$

Table 8. Roots of Normalized Bessel Polynomials 1st thru 6th Order Systems With 1-Second Settling Time [6]

The interconnection of the established linear control system and the nonlinear plant is shown in Figure 4 below. The system is nonlinear, but the system from v to w is approximated by the linear system defined by Equation 2.1.13.

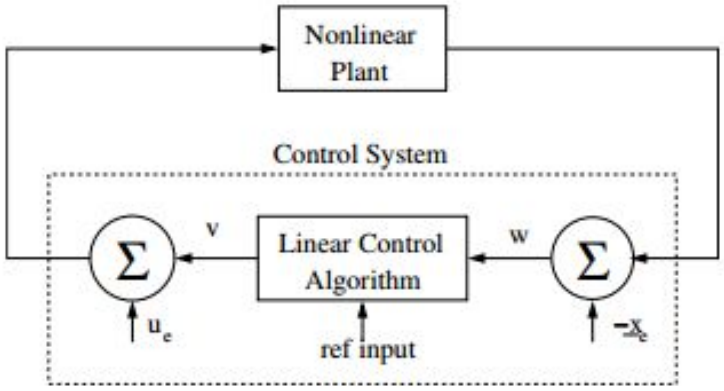

Figure 4. The connection between the nonlinear plant and linear control algorithm.

Here the equilibrium state vector x_e is subtracted from the measured state vector to yield w, the vector of state variable deviations, and the equilibrium plant input u_e is added to the output v. The resulting combination is a linear control algorithm which governs the plants deviations from equilibrium.

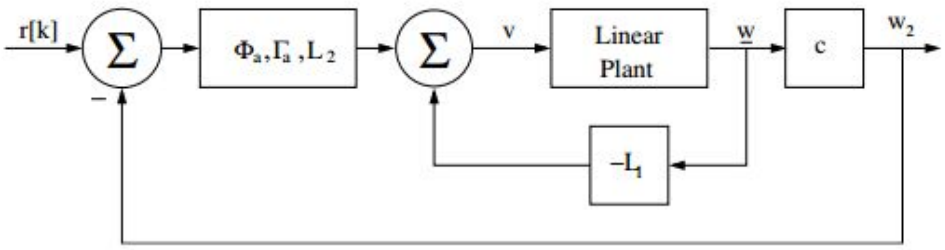

Figure 5. A tracking system for the linear plant model.

This basic loop outlined in Figure 5 shows the cascade structure of the linear plant with the additional dynamics needed for this problem. The reference input r[k] specifies the deviation of the liquid level in tank 2 from the value used to linearize the model. In order to apply this algorithm to the nonlinear plant the actual state variables must be converted to deviations from equilibrium as in Figure 4. Likewise the plant input v must be converted from a deviation term to the actual total value of pump voltage by adding u_e prior to being processed through the plant. Thus the complete tracking system follows Figure 6:

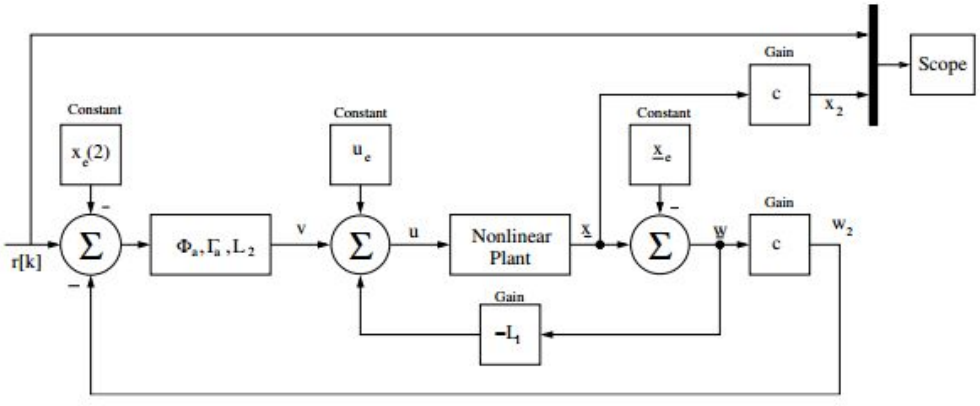

Figure 6. Tracking system applied to the nonlinear plant.

From Figure 6 it can be shown that the input to the plant is represented by:

$$u[t] = u_e + L_2 x_a[t] - L_1 w[t] \tag{3.1.7}$$

Here u_e represents the pump voltage associated with the equilibrium height in the

tanks, x_a is the state variable of the additional dynamics and $w[t]$ is the deviation of the state variables from equilibrium. Further examination of the control loop reveals that the initial value of the plant input is:

$$u[0] = u_e + L_2 x_a[0] - L_1 w[0] \tag{3.1.8}$$

Because both tanks are empty at the onset of system initiation $w[0] = -x_e$

$$u[0] = u_e + L_2 x_a[0] + L_1 x_e \tag{3.1.9}$$

Setting the initial plant input to zero and solving for the state variable of the additional dynamics ensures a smooth startup value for the plant input.

$$x_a[0] = -(u_e + L_1 x_e) * L_2^{-1} \tag{3.1.10}$$

3.2 Integrator Wind-up

As with any system there are limitations in its ability to respond to the demands of an applied command signal. In the case of the coupled-tank process the goal of the controller is to adjust the liquid height in the bottom tank by pumping fluid into the upper tank via supplying a range of voltages to the pump. To properly control this system the concept of *Integrator Wind-up* must be addressed.

The integrator is responsible for minimizing the set value error. The condition of integrator wind-up occurs when a system experiences a large change in set-point. The system is called to respond faster than its natural capacitance will allow resulting in large accumulation of error by the integrator [4]. This error grows large enough that even after the system has obtained its set value the integrator's *momentum* forces the system past the set-point. At this time error occurs in the opposite direction and the integrator finally begins to *unwind*. The overall result is an overshoot type scenario, which is an undesirable characteristic in matters of control.

The coupled-tank process demands set-points in discrete time and thus two physical limitations of the system become immediately apparent. The first of which deals with the range of voltage that the pump is able to accommodate. The second pertains to the maximum amount of liquid the tanks, specifically the upper tank is able to hold.

3.2.1 Pump Saturation

The Quanser Coupled-Tank system is supplied with a single electric powered pump whose power amplifier operates on a range of 0 to 22 volts. This voltage range sets a limit on the control systems ability to control the level of liquid in the lower tank. At one extreme the tracking system could command an input pump voltage higher than 22 volts in its attempt to mandate tank level under the specified settling time. This scenario commonly appears when a rapid increase in tank fluid height is required. A good technique to combat this problem is to set a threshold, from here on referred to as U_{max}, on the total input voltage $u[t]$ to the plant. This solution is not without its own faults as will be discussed in Section 3.3.

At the other extreme the tracking system could command a negative input value below that of 0 volts. This circumstance could occur if a drastic drop in tank fluid height is required. The tracking system would be attempting to feed a negative input value to the plant in the hopes of causing a vacuum to remove liquid at a faster rate than that of gravity alone. This of course is beyond the capabilities of the physical system. As such a second threshold must be implemented to limit all negative commanded values of $u[t]$ to a constant value of 0.

3.2.2 Tank Level Saturation

The second major limitation on the Coupled-Tank system presents itself in the upper tank's fluid capacity. The arrangement of the Quanser Two Tank Module is such that both the upper and lower tanks have an identical volume with orifices located at the bottom of each tank to facilitate as drains. These orifices are able to be adjusted in diameter allowing for increased and decreased draining for each tank, respectively. When a drastic increase in fluid height is commanded in the bottom tank a rapid inflow of fluid is introduced to the upper tank. Because the flow into the tank can be much greater than the flow out, due to orifice size, a scenario can occur where the tracking system commands a higher height in the upper tank than is physically possible. This is referred to as tank level saturation.

While the tracking system is merely performing its best to track the second tank height the physical system has reached its peak. As before with the saturation of the pump the solution to this problem relies on setting a constant value for the input to the plant, when the upper tank is commanded beyond its maximum value. This constant value, named U_{ssmax}, is the pump voltage at which the upper tank obtains a steady state height that coincides with the maximum height allowed in the tank. This value can be calculated provided the α coefficient of the orifice and β coefficient of the pump are known. Referencing the first line of Equation 2.1.4:

$$0 = \beta_1 u_e - \alpha_1 \sqrt{2g x_e(1)}$$

This equation describes the equilibrium upper tank height at steady state. Modifying the equation for the maximum allowable tank height, $x_{max}(1)$ instead of equilibrium height alters the equation as follows:

$$0 = \beta_1 U_{ssmax} - \alpha_1 \sqrt{2g x_{max}(1)} \tag{3.2.1}$$

Solving for U_{ssmax} yields:

$$U_{ssmax} = \frac{\alpha_1 \sqrt{2g x_{max}(1)}}{\beta_1} \tag{3.2.2}$$

It is important to note that $x_{max}(1)$ must be slightly less than the physical maximum tank height of the CTP. This is due to the loop implemented in the smart integrator. Performing this step avoids an infinite loop.

3.3 Anti-Windup Scheme

As speculated in Section 3.2.2 the method used for limiting the saturation of the input $u[t]$ is not without flaw. While this technique does address the case where the pump has been commanded beyond its maximum range it does not consider the previous portion of control which mandated the command. For this case an anti-windup scheme must be implemented. Here anti-windup refers to any measures taken to provide local feedback that make the controller stable alone when the main loop is opened by signal saturation [7]. Specifically this pertains to the x_a state variable of the additional dynamics. Under normal situations, i.e. those without saturation, the x_a variable is updated through the feedback loop specifying the change in deviation from equilibrium. The controller then looks at this updated state variable and adjusts the input voltage $u[t]$ accordingly to force the continued *tracking* of the system.

With the previous threshold scheme the normal order is disrupted by simply mandating the input to be a constant. The x_a state variable must then be properly updated to reflect the desired change in the control system. Standard calculation of x_a would involve the previous iteration of the state variable, $x_a old$ summed with the current total deviation from equilibrium signal e. Because the problem encountered is an overwhelming demand for higher input, the best solution is to adjust x_a in a manner that will bring the controller back into the acceptable range faster than would happen naturally. This is achieved by first calculating

the difference from the commanded input voltage and that set by the saturation threshold. The difference of these values is then scaled by an experimentally found L_3 gain [7]. Subtracting this product from the value of $x_a old$ yields the updated state variable x_a.

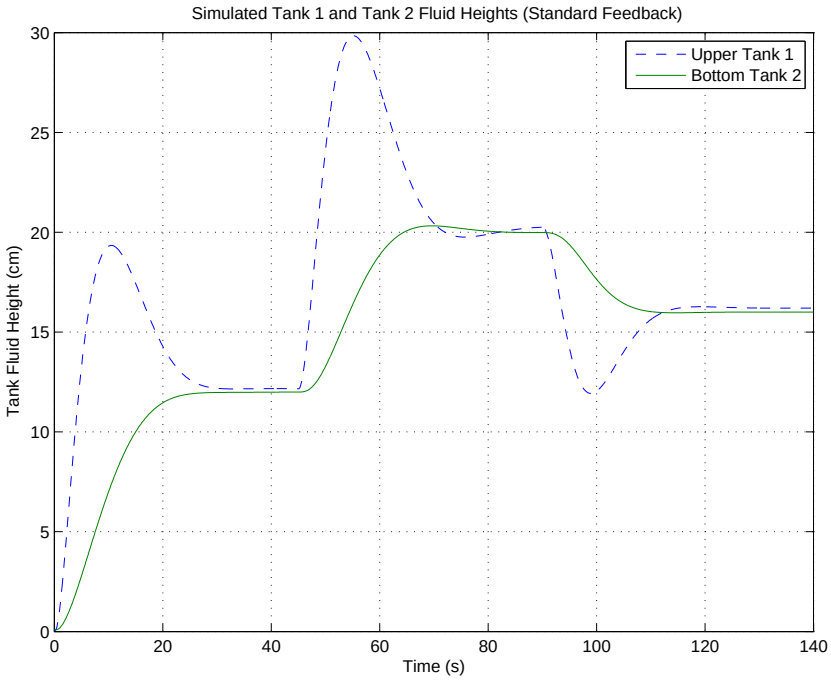

Figure 7. Simulated tank heights without physical limits.

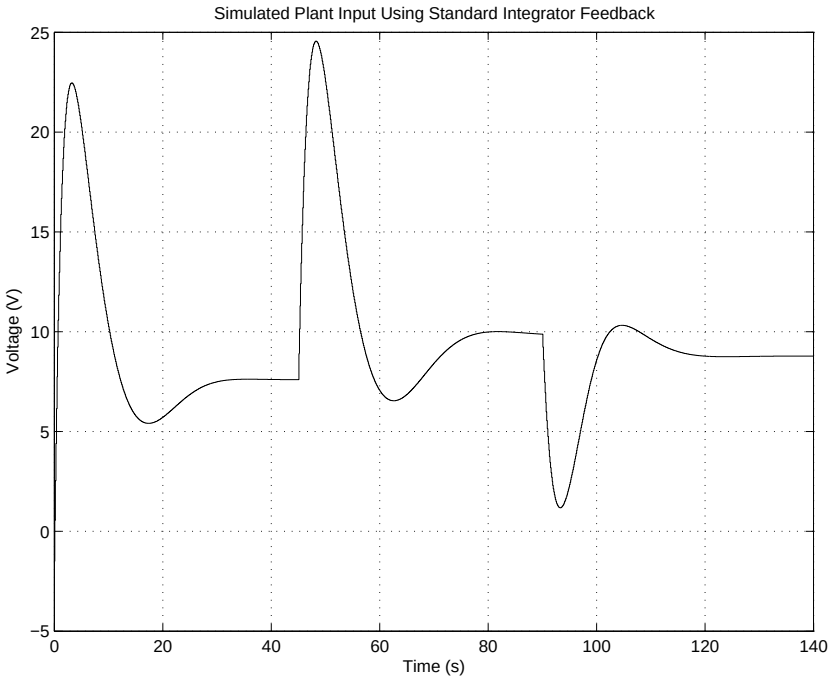

Figure 8. Simulated plant input with no consideration for physical limits.

As a starting point a simulation is performed using the same parameters calculated in Chapter 2. In this simulation the bottom tank received a series of desired height step commands starting from empty and in series from 12cm to 20cm to 16cm at 45 second intervals respectively. This simulation uses the standard integrator where the x_a variable is updated with the error signal e and operates as if no physical limitations exist. The system tracks the Tank 2 height exceptionally well as seen in Figure 7. However this figure also demonstrates the concept discussed in Section 3.2.2, regarding tank saturation. The control system commands the upper tank to obtain a 30 cm level when the accepted safe limit is physically 28 cm. The accompanying Figure 8 showcases the plant input or pump voltage commanded during the same simulation. As mentioned in Section 3.2.1 the maximum allowable pump voltage is 22 volts, whose limit is exceeded twice during this simulation.

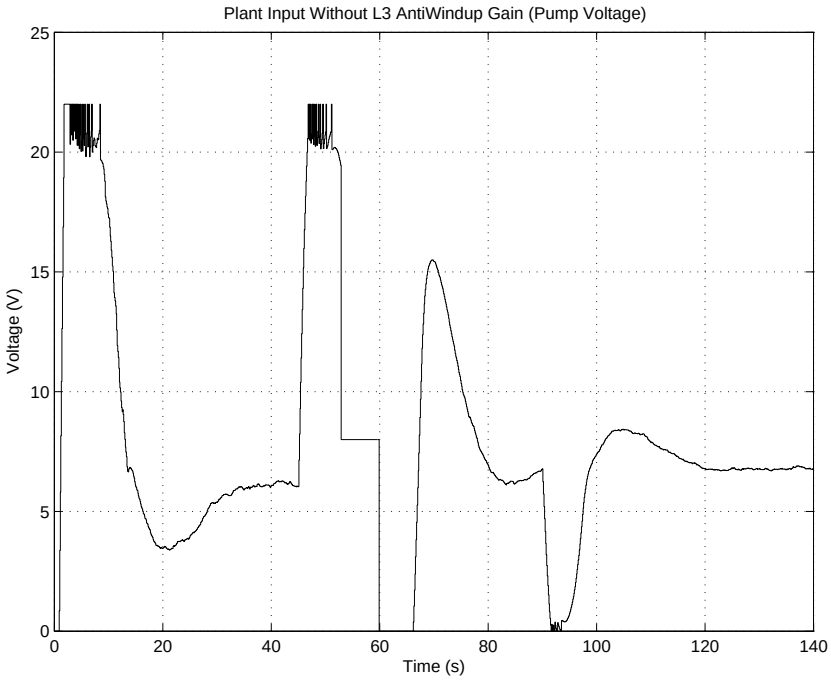

Figure 9. Plant input with physical limits and without xa updated.

A first attempt at remedying the saturations observed in simulation would be to simply add limits to the integrator in order to bring the simulation closer to the real system. Setting constant values for the pump voltage does not fully address the situation as the additional dynamics must be dealt with. Figure 9 demonstrates the behavior of the plant input when the x_a variable is not updated in times of saturation and simply recycles the previous x_a value. Notice the plant input's initial ramp up to fill the completely empty tank. The commanded pump voltage exceeds the 22 volt threshold and a oscillation of signal is experienced, which continues until the tank obtains the desired 12cm height and the commanded input falls well below the threshold. At 45 seconds the second change in set-point occurs once again resulting in a full pump value condition. This time however the condition is short lived as the upper tank begins to saturate and the Smart Integrator implements its U_{ssmax} threshold, seen here at approximately 8 volts. In comparison Figure 10 demonstrates the effectiveness of the L_3 gain technique

when all other parameters are kept constant. This figure was taken from the same experiment used to produce Figure 15 and 16 at the end of this chapter.

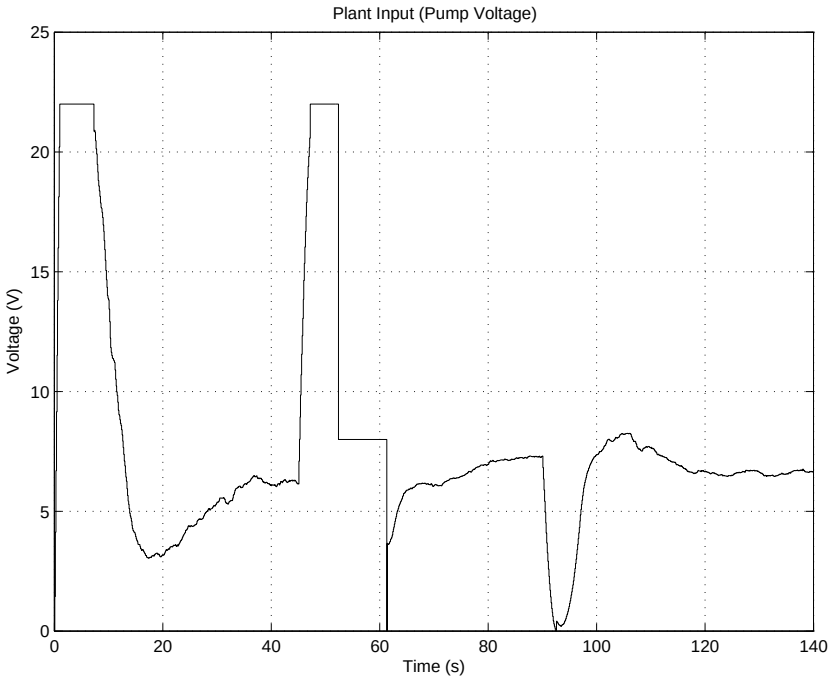

Figure 10. Input to plant using L3 antiwindup gain CTP.

3.4 Application to Hardware - Simulink

The overall application of the previously mentioned control scheme for the CTP is outlined below in Figure 11. The tracking system described by this block diagram was constructed using a companion package to Matlab, referred to as Simulink. This program allows predetermined values and equations that are setup in standard Matlab syntax to be pictorially represented as a feedback diagram. As a result once the overall control algorithm has the correctly calculated gains Simulink has the provisions to allow review of the systems performance via simulation. More importantly the tracking system produced by this diagram can be compiled by Simulink into C+ programming language and externally downloaded onto the desired hardware.

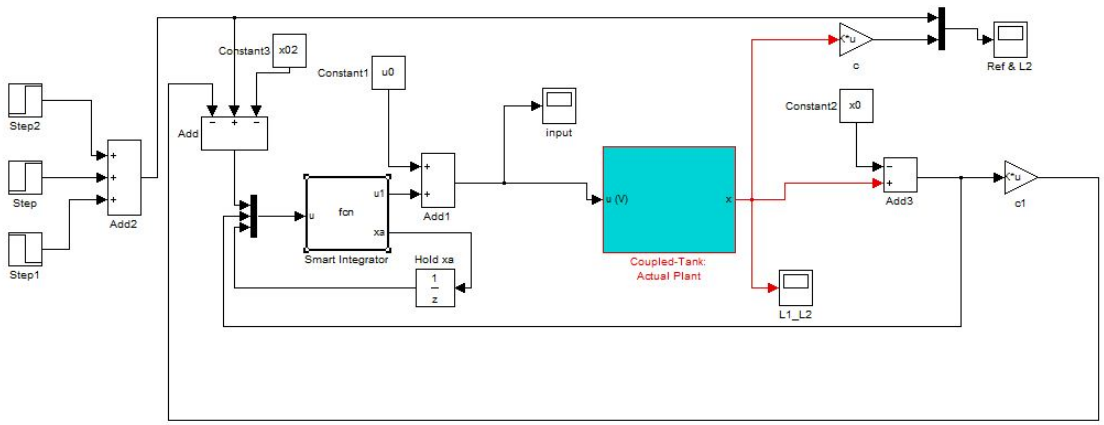

Figure 11. Block Diagram of Tracking System in Simulink for CTP.

Notice here the initial step command inputs which dictate the desired tank fluid heights at specified time intervals. The step commands are first brought to a summation junction where the deviation from the lower tank equilibrium height is found. This value is the *error* signal from equilibrium or e which becomes multiplexed with portions of the feedback loop prior to being input to the *Smart Integrator*.

The Smart Integrator function box in this diagram represents the implementation of control law Equation 3.1.7. As previously discussed in this chapter there exist certain cases where the use of 3.1.7 has to be modified in order to account for pump and tank saturation. The tactics used in this function block help the integrator of the controller minimize its accumulation of error and therefore limit any overshoot behavior. The application of this method in Simulink is as follows:

```
function [u1,xa] = fcn(u, L1, L2, Ussmax, Umax, u0, L1_MAX_C)
%#eml
e=u(1); %Error signal
x=u(2:3); %State variables
xa_old=u(4); %Previous iteration of Additional Dynamics
du=L2*xa_old-L1*x; %Standard Control Law
L3=10.5; %Experimentally found L3 Gain

if x(1)>L1_MAX_C-15 %Upper Tank Level Saturation
    xa=xa_old;
    u1=Ussmax-u0;
elseif du+u0 > 0.95*Umax %Pump Saturation - Upper Limit (within 95%)
    xa=xa_old-L3*((du+u0)-Umax); %L3 Gain Anti Windup Scheme
    u1=Umax-u0;
elseif du+u0 < 0 %Pump Saturation - Lower Limit
    xa=xa_old-L3*((du+u0)-0);    %L3 Gain Anti Windup Scheme
    u1=-u0;
else
    xa=xa_old+e; %Standard Integrator Feedback
    u1=du;
end
```

Figure 12. Smart Integrator Function

The output of each case is the determined change in pump voltage u_1 and the updated additional dynamics state variable x_a. Notice here that x_a is held from each prior iteration through the integrator, renamed $x_a old$, to be used in calculation of the next additional dynamics state variable. The change in voltage u_1 is summed with the equilibrium voltage and fed to the hardware plant. From here the system reacts and pressure sensor voltages are pulled from the hardware plant in order to update the x_1 and x_2 state variables. The deviation from equilibrium tank height is then recalculated and looped back to adjust both the difference from the desired step command and the integrator's next iterative response.

A demonstration of the results of this chapter are represented here via simulation and experimentally. The parameters which outline the Quanser Coupled Tank Process are listed below.

$$\dot{\mathrm{x}} = \mathrm{Ax} + \mathrm{b}u$$

$$y = \mathrm{cx}$$

where

$$A = \begin{bmatrix} -0.055988 & 0 \\ 0.055988 & -0.057025 \end{bmatrix}, b = \begin{bmatrix} 0.24813 \\ 0 \end{bmatrix}, c = \begin{bmatrix} 0 & 1 \end{bmatrix}$$

With a sampling interval of $T = 0.1s$.

$$\Phi = \begin{bmatrix} 0.99442 & 0 \\ 0.0055673 & 0.99431 \end{bmatrix}, \Gamma = \begin{bmatrix} 0.024744 \\ 0.000069201 \end{bmatrix}, \Phi_a = 1, \Gamma_a = 1$$

A selected settling time of T_s =20 seconds results in the following poles, p_i:

$$p_i = \text{spoles} = s3/T_s = [-0.19834 \pm 0.18922i \quad 0.25047]$$

Mapping the poles with the ZOH formula yields:

$$\text{zpoles} = e^{p_i * T} = [0.98019 \pm 0.01855i \quad 0.97526]$$

Supplied with the aforementioned data Matlab's *place* returned the following gains:

$$L_d = [2.1179 \quad 9.9757 \quad 0.13191]$$

$$L_1 = [2.1179 \quad 9.9757], \quad L_2 = [0.13191]$$

Gain and phase margins were as follows for this design model:

$$\text{Upper Gain Margin} = 30.1\text{dB}$$

$$\text{Lower Gain Margin} = -30.1\text{dB}$$

$$\text{Phase Margin} = 67\text{degrees}$$

Results were gathered using the following step commands over a total of 140 seconds.

$$r(t) = 12, \quad 0 \leq t < 45s$$
$$20, \quad 45 \leq t < 90s$$
$$16, \quad 90 \leq t < 140s$$

Simulation Results

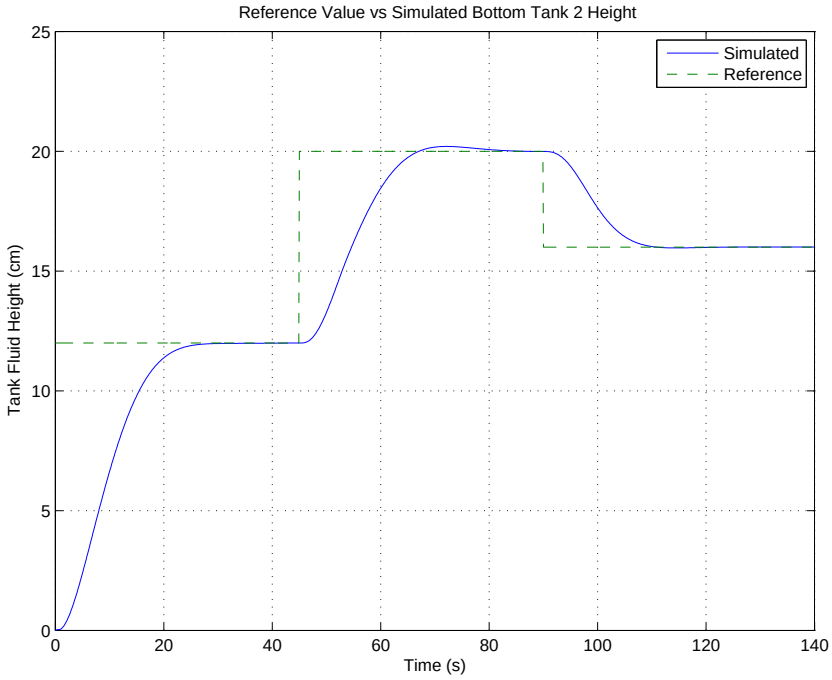

Figure 13. A comparison of commanded reference input to simulated fluid height CTP.

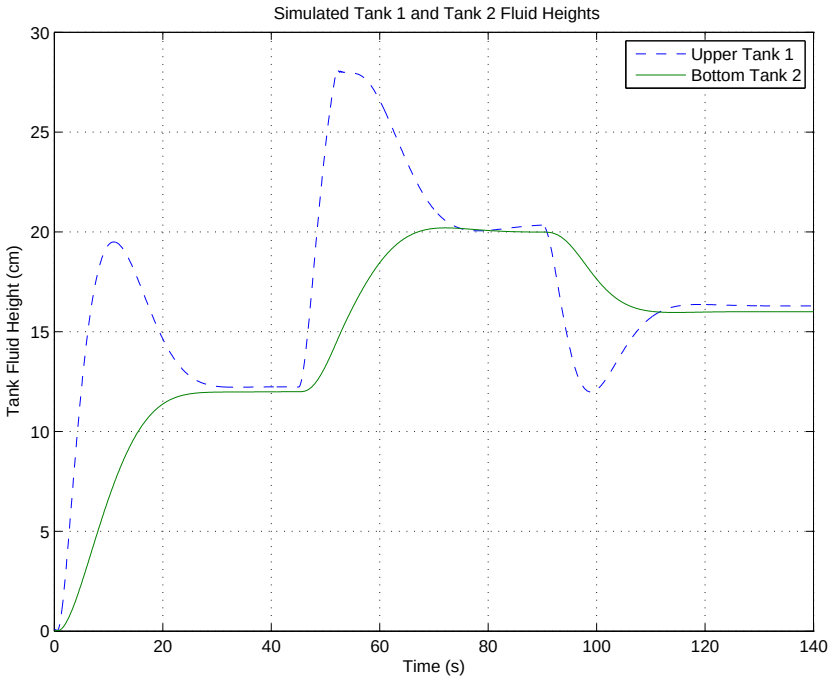

Figure 14. Simulated comparison of tank fluid heights CTP.

Experimental

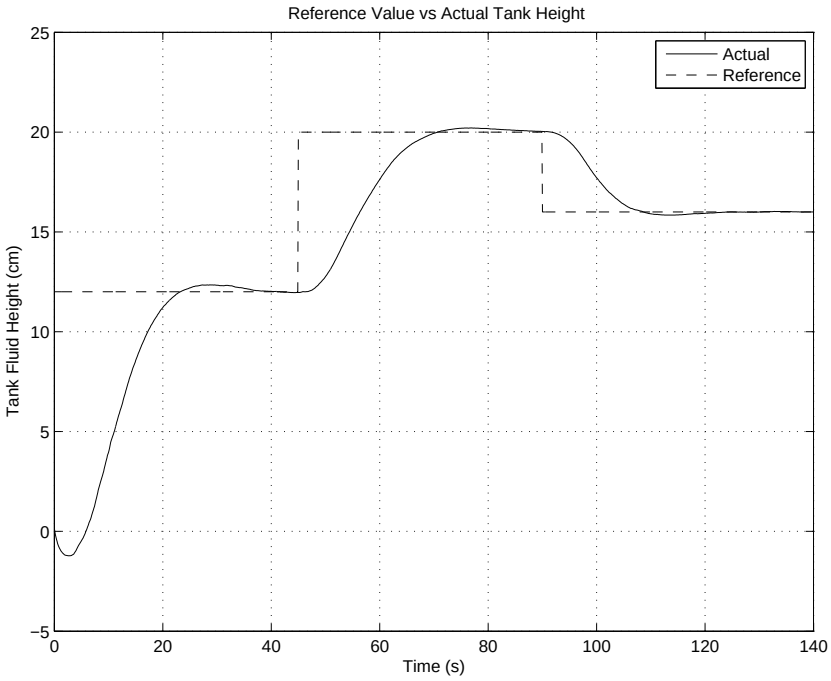

Figure 15. A comparison of commanded reference input to actual fluid height CTP.

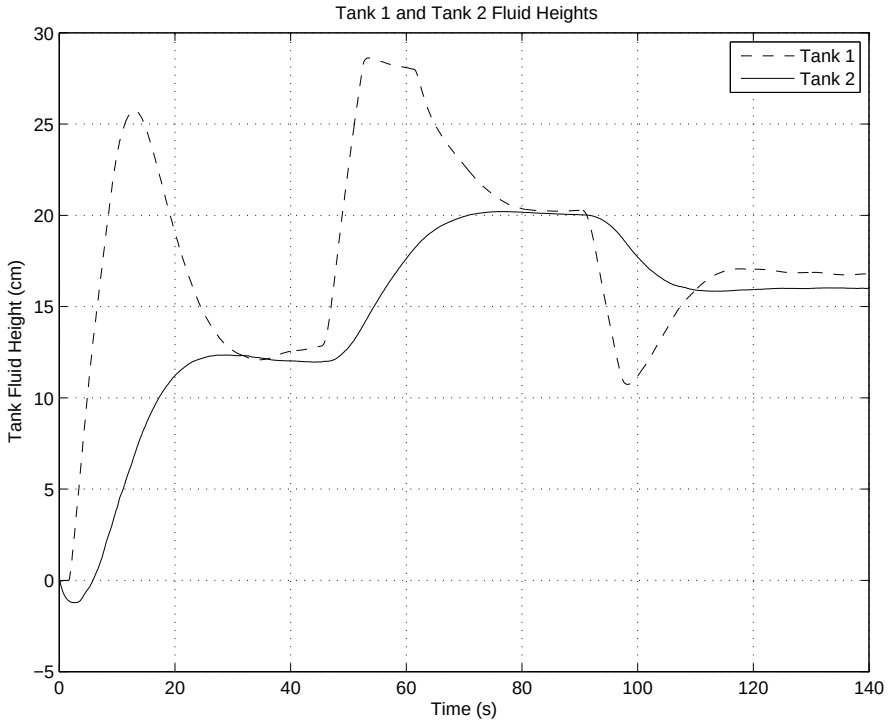

Figure 16. Actual comparison of tank heights during experiment CTP.

CHAPTER 4

Quadruple-Tank Process Control

4.1 Higher Order State Feedback Tracking System

As introduced in the coupled tank process a linear state feedback tracking system provides the desired level of control needed to effectively command tank fluid height. The same basic architecture can be transplanted into the quadruple tank process with provisions to accommodate the higher order of the system. The quadruple tank process is representative of a Multiple-Input, Multiple-Output (MIMO) system and therefore has a level of complexity not found in the CTP. The defining difference here lies with the fact that in a multi-variable system there exist an infinite number of different feedback matrices L that yield a given set of closed-loop pole locations [6]. In contrast a SISO system has a unique L gain vector associated with a given set of closed loop pole locations. In multi-variable problems it is therefore necessary to consider the *robustness* of the control system with the selected L feedback gain matrices to ensure stability when inevitable model errors are present.

4.1.1 Multi-Variable State-Space Tracking System Architecture

Because the linear tracking system architecture described in Chapter 3 remains valid for the QTP, the zero-order hold equivalent model introduced in Equation 3.1.3 is also valid. Represented here in discrete time as:

$$x[k+1] = \Phi x[k] + \Gamma u[k] \tag{4.1.1}$$
$$y[k] = \mathrm{C}x[k]$$

This equation holds true with the understanding that it follows the order of the system, n, where the QTP is of the 4th order. This means that the matrices Φ

and Γ will increase rank respectively to the linearized state space model described in Equation 2.2.8.

For a multi-variable system the additional dynamics must be applied to each of the system's outputs. With each output the additional dynamics are replicated into a parallel system. The QTP has two outputs that are represented by the two bottom tanks and requires a two times replication. Therefore the additional dynamics used for the Coupled -Tank

$$\Phi_a = 1, \quad \Gamma_a = 1,$$

are replicated for two outputs to obtain,

$$\bar{\Phi} = \begin{bmatrix} 1 & 0 \\ 0 & 1 \end{bmatrix}, \bar{\Gamma} = \begin{bmatrix} 1 & 0 \\ 0 & 1 \end{bmatrix}. \tag{4.1.2}$$

The replicated additional dynamics $\bar{\Phi}$ and $\bar{\Gamma}$ form a similar relation to Equation 3.1.4 given by:

$$\begin{aligned} x_a[k+1] &= \bar{\Phi} x_a[k] + \bar{\Gamma} u[k] \\ y_a[k] &= \mathrm{C} x_a[k] \end{aligned} \tag{4.1.3}$$

Following the tracking system laid out in Chapter 3, when the replicated additional dynamics of Equation 4.1.3 are cascaded with the ZOH model of the plant, described in Equation 4.1.1, the result is a design model for the overall system.

$$\Phi_d = \begin{bmatrix} \Phi & 0 \\ \bar{\Gamma}_a \mathrm{C} & \bar{\Phi}_a \end{bmatrix}, \Gamma_d = \begin{bmatrix} \Gamma \\ 0 \end{bmatrix} \tag{4.1.4}$$

where

$$x_d[k] = \begin{bmatrix} x[k] \\ x_a[k] \end{bmatrix} \tag{4.1.5}$$

This design model allows calculation of the feedback gain matrix $\mathbf{L}$ which has $n+2$ columns, where $n = 4$ for the QTP. The matrix $\mathbf{L}$ is partitioned into the first 4 and last 2 columns to obtain feedback gain matrices L_1 and L_2.

Parameter	Value
α_1	0.010949
α_2	0.012142
α_3	0.0040214
α_4	0.0053157
β_1	0.21009
β_2	0.23525
β_3	0.079938
β_4	0.088820
g	981

Table 9. Parameter Values for the Quanser Lab Quadruple Tank Process

4.1.2 Closed-Loop Pole Placement

The QTP system with the additional integrator dynamics is a 6th-order system, and care must be taken when choosing the closed-loop pole locations. Closed loop pole locations must be chosen under certain guidelines as to encourage the best output of performance. These guidelines are published in [8] and demonstrate a solid basis for choosing the pole locations of any standard system. For a tracking system these rules recommend normalized Bessel poles, shown in Table 8, scaled by the settling time as an initial foundation. However rather than using Bessel poles for all pole locations the stated rules suggest examining the natural poles and zeros of the plant to see if they merit use as closed loop poles. The analog plant poles of the QTP system used in the simulation at the end of this Chapter are as follows:

$$[-0.06758 \quad -0.07438 \quad -0.03308 \quad -0.05201] \tag{4.1.6}$$

In order to be selected as a closed loop pole the plant poles must be sufficiently damped in nature, that is they must have a real part which lies to the left of a first order Bessel pole divided by the desired settling time. The desired settling time for this QTP system is $Ts = 25s$. Therefore, sufficiently damped plant poles are those that lie to the left of $s1/T_s = -0.1848$. Under these given constraints none of the analog plant poles are a valid choice as closed loop pole locations.

The second applicable guideline for a tracking system recommends the selection of "slow", stable zeros of the plant for use as closed loop poles. The criteria for such zeros is that their real part be negative and lie to the right of $4 * s1/T_s = -0.7392$. Zeros of the plant were calculated to be:

$$[-0.06090 \quad -0.02419] \tag{4.1.7}$$

Because both zeros satisfy the criteria they are deemed eligible for examination as closed loop poles. From inspection it has been found that a slight modification of these poles to -0.0575 and -0.0225 results in optimum performance in both simulation and experimentation. The remaining poles will default to normalized Bessel poles as performed in the CTP. The following vector represents all six poles needed for the QTP with a settling time of $Ts = 25s$:

$$p_i = [-0.0575 \quad -0.0225 \quad s4/Ts] \tag{4.1.8}$$

As the QTP is a tracking system in discrete time all poles must be mapped into the z-plane using the ZOH pole mapping formula. This formula takes the selected poles represented by p_i and multiplies them by the sampling interval T before finally taking their exponential. This is represented in the following formula:

$$e^{p_i T} \tag{4.1.9}$$

4.1.3 Robust Feedback Gain Calculation

In Chapter 3 after having constructed the dynamic model and selected the desired closed loop poles, the feedback gains were calculated using the *place* function of Matlab. As previously mentioned, with a multi-variable system there exists an infinite number of feedback gain matrices that can be formulated from the same set of desired closed loop poles. While the *place* function will work with good results for this system time must be taken to examine the robustness of the overall system when these gains are used. Perturbation to the system can be caused by model errors and therefore a level of robustness must be ladened within the control system to account for the inaccuracies associated with modeling the dynamics of the system.

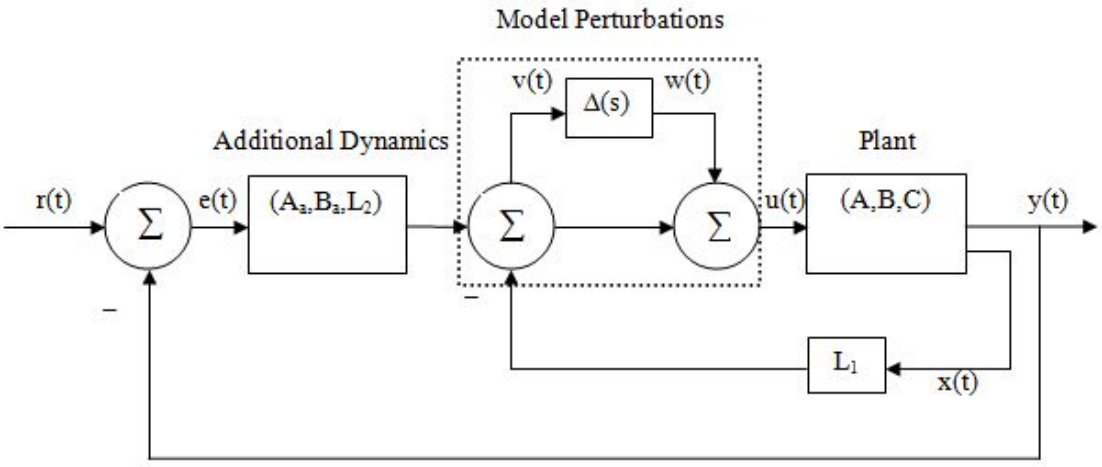

Figure 17. Model perturbation in state feedback tracking system.

In order to perform this examination a discussion of model perturbation and the small gain theorem must be introduced [9]. The diagram in Figure 17 represents a state-feedback tracking system with input-multiplicative plant perturba-

tion. This closed loop system is said to be stable when $\Delta(s) = 0$. This then implies that the system will remain stable as long as all model perturbations satisfy:

$$||\Delta(s)||_\infty < \delta_1 \tag{4.1.10}$$

Here the system infinity norm is:

$$||\Delta(s)||_\infty = sup_\omega \bar{\sigma}(\Delta(j\omega)) \tag{4.1.11}$$

$$\bar{\sigma}(\mathbf{M}) = \text{maximum singular value of } \mathbf{M}$$

The value δ_1 represents the reciprocal of the infinity norm of the system from w(t) to v(t) [10]. From the tracking system shown the system from w(t) to v(t), with r(t) set to zero, or $\mathbf{G}$(s) can be described in state-space form as:

$$\begin{bmatrix} \dot{x} \\ \dot{x_a} \end{bmatrix} = \begin{bmatrix} A - BL_1 & BL_2 \\ -B_aC & A_a \end{bmatrix} \begin{bmatrix} x \\ x_a \end{bmatrix} + \begin{bmatrix} B \\ 0 \end{bmatrix} \text{w} \tag{4.1.12}$$

$$v = \begin{bmatrix} -L_1 & L_2 \end{bmatrix} \begin{bmatrix} x \\ x_a \end{bmatrix}$$

The stability robustness bound for this tracking system is then given by:

$$\delta = \frac{1}{||\mathbf{G}(s)||_\infty} \tag{4.1.13}$$

This robustness norm is then used to gage how well the model will remain stable under a certain level of perturbation. Generally speaking the larger this number the larger the inaccuracy the controller is able to handle while keeping the system stable. The accepted region for a robustly stable system is as follows:

$$0.5 \leq \delta_1 < 1 \tag{4.1.14}$$

Utilizing Matlab's *place* function to calculate feedback gains reveals a $\delta_1 = 0.8451$ for the simulated QTP calculated at the end of this chapter. This illustrates that the system will have more than sufficient robustness to function even in the face of model perturbation.

4.2 QTP Simulation

A demonstration of the results of this chapter are represented here via simulation. The parameters which outline the Quanser Quadruple Tank Process are outlined in Table 9.

$$\dot{\mathrm{x}} = \mathrm{Ax} + \mathrm{b}u$$

$$y = \mathrm{cx}$$

where

$$A = \begin{bmatrix} -0.06758 & 0 & 0.03308 & 0 \\ 0 & -0.07438 & 0 & 0.05202 \\ 0 & 0 & -0.03308 & 0 \\ 0 & 0 & 0 & -0.05202 \end{bmatrix}, b = \begin{bmatrix} 0.21009 & 0 \\ 0 & 0.23525 \\ 0 & 0.079938 \\ 0.088820 & 0 \end{bmatrix}$$

$$c = \begin{bmatrix} 1 & 0 & 0 & 0 \\ 0 & 1 & 0 & 0 \end{bmatrix}, \quad u_e = \begin{bmatrix} 6 \\ 6 \end{bmatrix}$$

With a sampling interval of $T = 0.1s$.

$$\Phi = \begin{bmatrix} 0.9933 & 0 & 0.003291 & 0 \\ 0 & 0.9926 & 0 & 0.005169 \\ 0 & 0 & 0.9967 & 0 \\ 0 & 0 & 0 & 0.9948 \end{bmatrix}, \quad \Gamma = \begin{bmatrix} 0.02094 & 0.00001318 \\ 0.00002300 & 0.02344 \\ 0 & 0.007981 \\ 0.008859 & 0 \end{bmatrix}$$

$$\Phi_a = \begin{bmatrix} 1 & 0 \\ 0 & 1 \end{bmatrix}, \Gamma_a = \begin{bmatrix} 1 & 0 \\ 0 & 1 \end{bmatrix}$$

A selected settling time of T_s =25 seconds results in the following poles, p_i:

$$p_i = \text{spoles} = [-0.0225 \quad -0.0575 \quad -0.1606 \pm 0.2029i \quad -0.2211 \pm 0.0662i]$$

Mapping the poles with the ZOH formula yields:

$$\text{zpoles} = e^{p_i} = [0.9978 \quad 0.9943 \quad 0.9839 \pm 0.01996i \quad 0.9781 \pm 0.006476i]$$

Supplied with the aforementioned data Matlab's *place* returned the following gains:

$$L_1 = \begin{bmatrix} 0.7046 & -0.01568 & 0.5913 & 2.123 \\ 0.3090 & 0.8001 & 1.138 & 0.4038 \end{bmatrix}, \quad L_2 = \begin{bmatrix} 0.02566 & -0.0008726 \\ -0.006911 & 0.02419 \end{bmatrix}$$

Using *place* for gain calculation returned a system with robustness norm $\delta = 0.8451$.

Results were gathered using the following step commands over a total of 180 seconds.

$$r(t) = \begin{bmatrix} 12 \\ 12 \end{bmatrix}, \quad 0 \leq t < 60s$$
$$\begin{bmatrix} 20 \\ 20 \end{bmatrix}, \quad 45 \leq t < 120s$$
$$\begin{bmatrix} 16 \\ 16 \end{bmatrix}, \quad 90 \leq t < 180s$$

Simulation Results

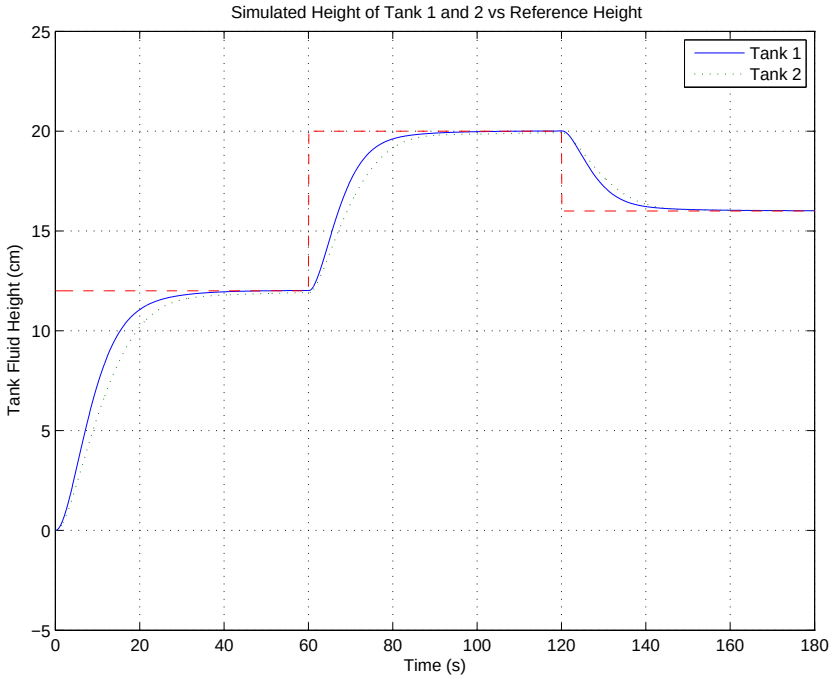

Figure 18. A simulated comparison of commanded reference input to tank fluid height QTP.

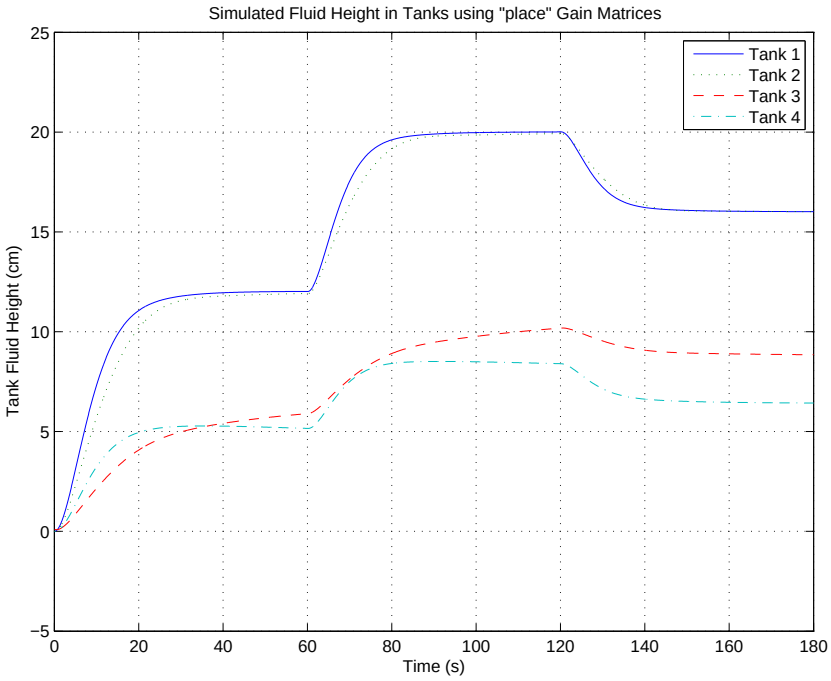

Figure 19. Simulated tank fluid height responses QTP.

Experimental Results

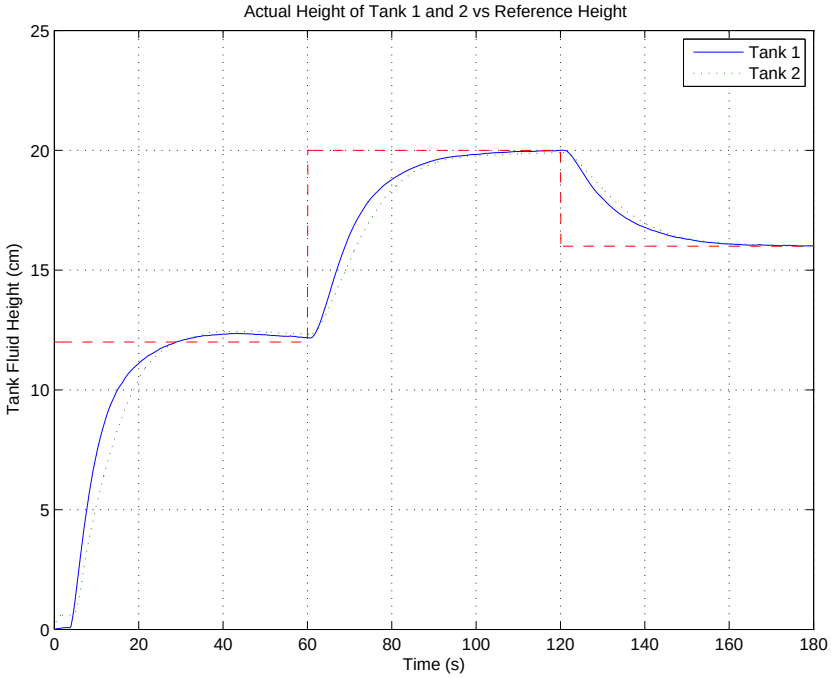

Figure 20. Actual comparison of commanded reference input to tank fluid height QTP.

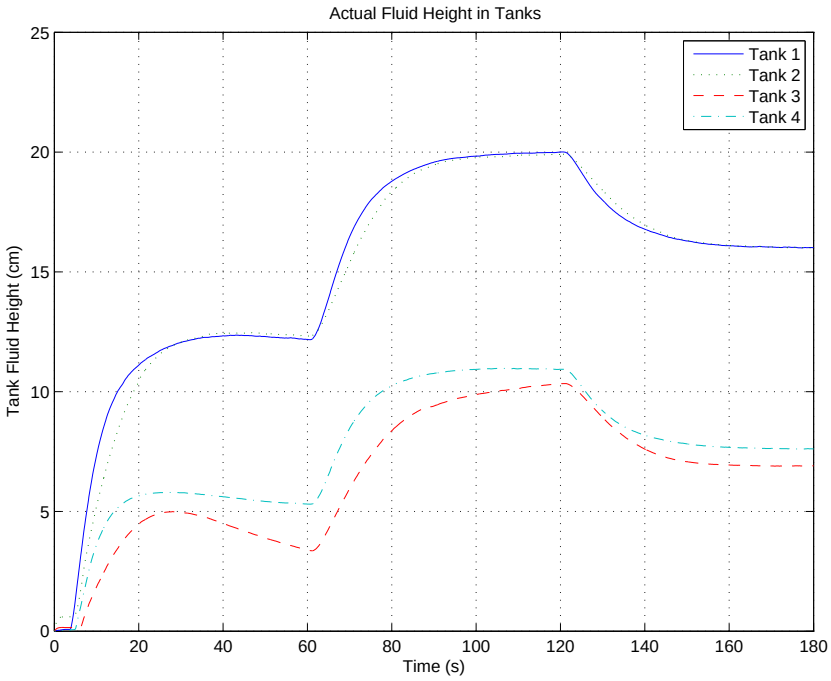

Figure 21. Actual tank fluid height responses QTP.

CHAPTER 5

Conclusion and Recommendations

Given the state-space tracking system architecture demonstrated in this study the prowess of this type of control over the QTP has been made apparent. The digital state-space control employed in this thesis effectively tracked the tank fluid heights under the mandated constraints. The controller performed this task using several techniques to combat many difficulties associated with the QTP including non-linear system dynamics, integrator windup and actuator saturation. With a substantial robustness from proper pole placement the stability and phase margins reveal a system that has ample performance over a considerable bandwidth. This is key when considering the perturbations that could arise should outside forces change the plant model or the ability of the physical system to respond to the controller.

Future work regarding the control the tank processes systems should contemplate the benefits of gain scheduling. This method establishes a range of equilibrium or set points for which traditional feedback gains can be calculated. The benefit to this method is that the control system does not have to rely on one set of gains focused around one equilibrium and instead can actively update the gains depending on the systems position to optimize control [11]. This method could offer further enhancement of the QTP considering the linearized dynamics and a viable addition to the techniques already discussed.

Further advancements in the study of the QTP should also focus on techniques to deal with the Non-Minimum Phase behavior that occurs in a specified range of inlet pump flow. The configuration used in this study was of the minimum phase type. With minor modifications to the apparatus one could study this peculiar

characteristic of the QTP and make provisions from a state-space approach to attempt acceptable performance under the given constraints. Non-minimum phase in the QTP occurs when the rate of inlet flow to the upper tanks exceeds that of the inlet flow to the bottom tanks. As a result of this the non-minimum configuration is significantly harder to control and requires settling times an order of magnitude larger than a minimum phase counterpart.

It is important to note that given the dynamics of the apparatus it is essential that to yield good experimental results that the apparatus be calibrated correctly and often. The pressure sensors in both the CTP and QTP are temperamental to changes in climate, such as barometric pressure changes. If not properly calibrated the system will exhibit poor performance most likely in the form of steady state error regarding the tank heights. Calibration of these sensors has been discussed in Chapter 2, but it is the prominent culprit for control system failure in the tank processes. With uncalibrated sensors the input to the control system is flawed, and although the plant dynamics are still valid supplying the control law with false readings will incur a performance error outside the scope of the tracking system.

LIST OF REFERENCES

[1] K. H. Johansson, "The-quadruple-tank process: A multivariable laboratory process with an adjustable zero," in *IEEE Transactions on Control Systems Technology*.

[2] K. H. Johansson, "Teaching multivariable control using the quadruple-tank process," in *Proceedings IEEE Conference on Decision and Control*.

[3] R. K. Qamar Saeed, Vali Uddin, "Multi-variable predictive PID control for the quadruple tank process," in *World Academy of Science, Engineering and Technology*.

[4] L. Zaccarian and A. R. Teel, *Modern Anti-windup Synthesis*. Princeton,New Jersey: Princeton Uniiversity Press, 2011.

[5] E. Davison and A.Goldenburg, "Robust control of a servomechanism problem: the servo compensator," *Automatica*, vol. 11, pp. 461–471, 1975.

[6] R. J. Vaccaro, *Digital Control: A State-Space Approach*. New York,NY: McGraw-Hill, 1995.

[7] J. D. P. Gene F. Franklin and A. Emami-Naeini, *Feedback Control of Dynamic Systems-Fifth Edition*. Upper Saddle River,New Jersey: Pearson Prentice Hall, 2006.

[8] R. J. Vaccaro, "An optimization approach to the pole-placement design of robust linear multivariable control systems," in *Proceedings 2014 IEEE American Control Conference*.

[9] J. Burl, *Linear Optimal Control*. Menlo Park, CA: Addison Wesley Longman, 1999.

[10] S. Skogestad and I. Postlethwaite, *Multivariable Feedback Control: Analysis and Design, 2nd ed.* Chichester, England: John Wiley and Sons, 2005.

[11] G. K. Nicholas Kottenstette, Joseph Porter and J. Sztipanovits, "Discrete-time ida-passivity based control of coupled tank processes subject to actuator saturation," in *3rd International Symposium on Resilient Control Systems*.

BIBLIOGRAPHY

Burl, J., *Linear Optimal Control*. Menlo Park, CA: Addison Wesley Longman, 1999.

Davison, E. and A.Goldenburg, "Robust control of a servomechanism problem: the servo compensator," *Automatica*, vol. 11, pp. 461–471, 1975.

Gene F. Franklin, J. D. P. and Emami-Naeini, A., *Feedback Control of Dynamic Systems-Fifth Edition*. Upper Saddle River,New Jersey: Pearson Prentice Hall, 2006.

Husek, P., "Decentralized pi controller design based on phase margin specifications," in *IEEE Transactions on Control Systems Technology*.

Johansson, K. H., "Teaching multivariable control using the quadruple-tank process," in *Proceedings IEEE Conference on Decision and Control*.

Johansson, K. H., "The-quadruple-tank process: A multivariable laboratory process with an adjustable zero," in *IEEE Transactions on Control Systems Technology*.

Nicholas Kottenstette, Joseph Porter, G. K. and Sztipanovits, J., "Discrete-time ida-passivity based control of coupled tank processes subject to actuator saturation," in *3rd International Symposium on Resilient Control Systems*.

Qamar Saeed, Vali Uddin, R. K., "Multi-variable predictive PID control for the quadruple tank process," in *World Academy of Science, Engineering and Technology*.

Specialty Experiment: PI-plus-Feedforward Water Level Control, Coupled-tank control laboratory-instructor manual ed., Quanser Consulting, document Number: 559, Revision: 05.

Specialty Experiment: PI-plus-Feedforward Water Level Control, Coupled-tank control laboratory-student handout ed., Quanser Consulting, document Number: 558, Revision: 05.

Specialty Experiment: PI-plus-Feedforward Water Level Control, Coupled water tank experiments ed., Quanser Consulting, CTP Experiments.

Skogestad, S. and Postlethwaite, I., *Multivariable Feedback Control: Analysis and Design, 2nd ed.* Chichester, England: John Wiley and Sons, 2005.

Uren, K. and van Schoor, G., *Advances in PID Control: Predictive PID Control of Non-Minimum Phase Systems*. Rijeka, Croatia: Intech, 2011.

Vaccaro, R. J., "Digital control of coupled water tanks," ELE 458 Lab 5.

Vaccaro, R. J., "An optimization approach to the pole-placement design of robust linear multivariable control systems," in *Proceedings 2014 IEEE American Control Conference*.

Vaccaro, R. J., *Digital Control: A State-Space Approach*. New York,NY: McGraw-Hill, 1995.

Vaccaro, R. J., "Digital control of quadruple-tank process," Fall 2012, ELE 503 Final Project.

Vanamane, V. and Patel, N., "Modeling and controller design for quadruple tank system," in *Proceedings of the Intl. Conference on Advances in Computer, Electronics and Electrical Engineering*.

Zaccarian, L. and Teel, A. R., *Modern Anti-windup Synthesis*. Princeton,New Jersey: Princeton Uniiversity Press, 2011.